RSC Advances

Developing acetylcholinesterase-based inhibition assay by modulated synthesis of silver nanoparticles: Application for sensing of organophosphorus pesticides

Journal:	*RSC Advances*
Manuscript ID:	RA-ART-05-2015-010146.R1
Article Type:	Paper
Date Submitted by the Author:	27-Jun-2015

Complete List of Authors:	D, Nanda; VIT University, Centre for nanobiotechnology A, Rajeshwari; VIT University, Centre for nanobiotechnology Alex, Sruthi; VIT University, M, Sahu; IISC, Raichur, Ashok; IISc, Materials Engineering Chandrasekaran, N; VIT University, Centre for Nanobiotechnology Mukherjee, Amitava; VIT University, Centre for Nanobiotechnology

Developing acetylcholinesterase-based inhibition assay by modulated synthesis of silver nanoparticles: Application for sensing of organophosphorus pesticides

D. Nanda Kumar[1], A. Rajeshwari[1], S. A. Alex[1], M. Sahu[2], A.M. Raichur[2], N. Chandrasekaran[1], A. Mukherjee[1]*

[1] Centre for Nanobiotechnology, VIT University, Vellore, India

[2] Department of Materials Engineering, Indian Institute of Science, Bangalore, India

*Corresponding author

Dr. Amitava Mukherjee

Senior Professor & Deputy Director

Centre for Nanobiotechnology

VIT University, Vellore - 632014

Email: amit.mookerjea@gmail.com, amitav@vit.ac.in

Phone: 91 416 2202620

Fax: 91-416-2243092

ABSTRACT

A novel and highly sensitive sensing strategy for detection of organophosphorus compounds (OPs) based on the catalytic reaction of acetylcholinesterase (AChE) and acetylcholine (ATCh) during the modulated synthesis of silver nanoparticles (AgNPs) has been developed. The enzymatic hydrolysis of ATCh by AChE yields thiocholine (TCh), which induces the aggregation of AgNPs during synthesis, and the absorption peak at 382 nm corresponding to AgNPs decreases. The enzymatic reaction can be regulated by OPs, which can covalently bind to the active site of AChE and decrease the TCh formation, thereby decreasing the aggregation and significantly enhancing the absorption peak at 382 nm. The proposed system achieved good linearity and limit of detection of 0.078 nM and 2.402 nM for trichlorfon and malathion, respectively, by UV–visible spectroscopy. Further, the sensitivity of the proposed system was demonstrated through the determination of OPs in different spiked real samples. The described work shows the potential application for further development of a colorimetric sensor for other OP pesticide detection during the synthesis of AgNPs using enzyme-based assay.

Key words: Trichlorfon; Malathion; Acetylcholinesterase; Silver nanoparticles.

Introduction

In the earlier decades, the use of pesticides that contain organophosphorus compounds (OPs) and their derivatives were widely employed in agriculture because of their low persistence in the environment.[1] These compounds exhibit acute toxic effect on the human nervous system or can even cause nerve cell death by accumulation of acetylcholine.[2] These OPs have been employed as chemical warfare agents, thereby causing increased threat from terrorists also.[3] These facts highlight that there is an increasing concern on developing a simple, rapid, and sensitive strategy for the detection of OP compounds without any sophisticated instruments. In general, there are several analytical techniques that have been used for the detection of these compounds namely, HPLC,[4] mass spectroscopy[5], and gas chromatography.[6] The disadvantage of these methods is the requirement for expensive instrumentation with well-skilled personnel and inadequate detection limits.

On the other hand, metal and semiconductor nanoparticles (NPs) have gained more attention towards the biorecognition process due to their optical and electrical properties.[7] The silver nanoparticles (AgNPs) and gold nanoparticles (AuNPs) are extensively used because of their aggregation property in solution, which is dependent on the analyte concentration, and this in turn yields different-sized NPs with different light absorption capacities.[8,9] In recent years, NPs have been exploited as they promote the determination of OPs due to their rapid and sensitive response towards biorecognition elements. The use of NPs have great advantages, e.g. high sensitivity and responsiveness, low cost, easy to synthesis, and can be used as direct signal sources for the detection of OP pesticides.[10]

Several enzyme-based biosensors have been established based on amperometric techniques and colorimetric and fluorescence spectroscopy for the detection of OP group-containing pesticides

in the environment using NPs.[11-13] The enzyme AChE, which can be inhibited by these OP pesticides, can be employed to furnish a rapid analysis of OP pesticides. Phosphorylation of pesticides can destroy the OH bond of serine in AChE, and this has caused changes in the localized surface plasmon resonance (LSPR) of NPs as they interact with the end-product of the enzyme, which can be used to estimate the concentration of OPs.[14] Pavlov *et al.*, demonstrated the colorimetric detection of AChE inhibitor, 1,5-bis(4-allyldimethylammoniumphenyl)-pentane-3-one dibromide or paraoxon by the inhibition of AChE-mediated hydrolysis of acetothiocholine (ATCh), which affects the aggregation rate of gold nanoparticles (AuNPs).[15] He *et al.*, developed a simple, facile, and highly sensitive luminol-functionalized AgNP-based chemiluminescent (CL) sensor for organophosphate and carbamate pesticides. These sensors could recognize a concentration level of 24 μg mL^{-1} for five organophosphate and carbamate pesticides, including dimethoate, dipterex, carbaryl, chlorpyrifos and carbofuran.[16] Recently, Li et al., demonstrated that thiocholine-induced aggregation of AgNPs was found when AgNPs were added to a mixture of AChE and ATCh, and the aggregation of AgNPs was prevented by irreversible inhibition of AChE by the addition of dipterex in the range 0.25-37.5 ng mL^{-1}, and they achieved a limit of detection (LOD) of 0.699 nM.[17] All these methods were established after the synthesis, modification, and functionalization of NPs for detection of OP pesticides.

Recently, Pavlov *et al.*, (2014) reported the thiol-mediated stabilization of *in situ* generated, fluorescent CdS quantum dots (QDs) for the detection of AChE inhibitors like paraxon and galantamine with a limit of detection (LOD) of 0.06 nM and 115 nM, respectivley.[18] The large surface areas of QDs may reduce the luminescence activity [19] and reduce the quantum yield, which are the limitations of QDs.[20] The Pavlov *et al.*, (2009) group studied the modulated growth of Au-AgNPs for sensing of nerve gases like 1,5-bis(4-allyldimethylammoniumphenyl)pentan-3-

onedibromide or diethyl p-nitrophenyl phosphate (paraoxon) by enzyme inhibition method with an LOD of 4 nM, but the complexity in the formation of Au-Ag NPs system makes the method difficult to use.[21] Wang *et al.*, (2011) developed an electrochemical sensor by synthesizing an Au NP/cr-Gs hybrid on the surface of graphene nanosheets using poly(diallyldimethylammonium chloride) (PDDA) as a linker for self-assembling of cholinesterase for the ultrasensitive detection of paraoxon[22], but the time requirement for graphene oxide synthesis and the complicated fabrication process are the major disadvantages of this system.

The present work describes a novel strategy for the direct colorimetric detection of OP pesticides (AChE inhibitors, namely trichlorfon and malathion) using an enzyme-based method during the modulated synthesis of AgNPs by modified Creighton method (involving $AgNO_3$, $Na_3C_6H_5O_7$, and $NaBH_4$). The principle of this method is based on the aggregation of NPs in the presence of thiol-bearing compound, TCh, liberated by the enzymatic hydrolysis reaction, which in turn decreases the absorbance (at 382 nm in the UV–visible spectra) of AgNPs during synthesis. The addition of OP pesticide to this system irreversibly inhibits the AChE and significantly decreases the production of TCh molecule. Thus, the absorbance at 382 nm would again increase with the increasing concentrations of the OPs added. The proposed method was able to detect 0.1 nM of trichlorfon and 1 nM of malathion with a detection limit of 0.078 nM and 2.402 nM for trichlorfon and malathion, respectively. The probe achieved the lowest LOD for OP pesticide detection during the synthesis of AgNPs as compared with the other existing methods using NPs (Table 1). Summarizing, the major significance of the current study lies in its ability to determine more than one type of OP pesticides at very low concentrations in aqueous solution during the synthesis of AgNPs without the addition of any external linkers or seed solutions.

Experimental section

Chemicals

Analytical grade pesticides, trichlorfon (96.7%), and malathion (98.7%) were purchased from Sigma-Aldrich, India. Silver nitrate ($AgNO_3$), trisodium citrate dihydrate ($Na_3C_6H_5O_7.2H_2O$), and sodium borohydride ($NaBH_4$) were procured from SRL Pvt. Ltd (India). Acetylcholinesterase (AChE, from *Electrophorus electricus*) was obtained from Sigma-Aldrich, India. Ethanol (99.9%) was purchased from SD Fine Chemicals Ltd (India). Tris (hydroxymethyl) aminomethane (tris buffer) and acetylthiocholine iodide (ATChI) were obtained from Himedia Laboratories Pvt. Ltd (India).

Apparatus

Absorption spectra were recorded with a UV–visible absorption spectrometer (UV-2600, Shimadzu, Tokyo, Japan) and all the measurements were made in the spectral range from 200 to 800 nm. Transmission electron microscopy (TEM) measurements were performed using FEI Company Tecnai™, G^2 Spirit, BioTWIN at an accelerating voltage of around 120 kV. Dynamic light scattering (DLS) and zeta potential were performed using a particle size analyzer (NanoBrook 90Plus PALS Particle Size Analyzer, Brookhaven Instruments Corporation, USA). FT-IR spectra were recorded in the range of 600–4500 cm^{-1} using IR Affinity-1, Shimadzu, FT-IR spectrometer in KBr pellets.

Preparation of stock solutions

AChE and ATChI stock solutions were prepared using tris buffer solution (10 mM pH 7.4) and stored in the refrigerator at 4-5 °C when not in use. A stock solution of trichlorfon (10^{-3} M) was prepared in deionized water (Milli-Q), whereas malathion (10^{-3} M) was prepared freshly in ethanol, and further, the solutions were diluted with Milli-Q to the appropriate dilution for further experimental use. Aquaregia solution was used for the cleaning of all glassware apparatus, which was finally rinsed with Milli-Q water at least two times and dried in a hot-air oven. These analytical grade chemical reagents were used in all the experiments without further purification. Ultrapure deionized water (Milli-Q) obtained from Cascada Bio water (Pall Corporation, USA) was used throughout the experiments, unless stated otherwise.

Inhibition of AChE by trichlorfon and malathion

The inhibition of AChE was studied by using two different OP pesticides, trichlorfon and malathion (for chemical structure details see ESI in Fig. S1). The different concentrations of trichlorfon, from 0 to 1.2 nM (100 µL), and malathion, from 0 to 14 nM (100 µL), were incubated separately with the reaction mixture of 10 µL of AChE (100 mU mL^{-1}) and 20 µL of ATCh (0.1 mM) for 10 min at 37 °C, respectively. Then, 100 µL of $AgNO_3$ (1 mM) was added, followed by the addition of 50 µL of $Na_3C_6H_5O_7$ (1%) and 20 µL of $NaBH_4$ (10 mM) to each of the above reaction mixture, and the final volume of reaction mixture was adjusted to 1 mL with Milli-Q water. After that, the UV–visible spectra of the resulting sample mixture was recorded at room temperature and the linear calibration curve was plotted between different concentration of OPs and absorbance ratio (A/A_0). The whole experiment was carried out under pH 7.4±1, and no obvious change in the pH was observed in the system (AgNPs, AChE and ATCh) before and

after interaction with trichlorfon and malathion. The reaction pH was found to be within the range of 6.8-7.5.

Kinetic behavior

Different concentrations of trichlorfon (0.0, 0.2, 0.4, 0.8, and 1.0 nM) and malathion (0, 2, 4, 6, 8, and 10 nM) were added to the reaction mixture of AChE (10 µL, 100 mU mL^{-1}) and ATCh (20 µL, 0.1 mM) and the system containing, $AgNO_3$, $Na_3C_6H_5O_7$, and $NaBH_4$, and their absorption spectra (at 382 nm) were recorded at reaction times varying from 0 to 900 s. The rate constant for each pesticide concentration (trichlorfon and malathion) and the system without pesticides can be estimated by using the obtained kinetic data. For the kinetic analysis of the inhibition of AChE by OP pesticides at room temperature (25 °C ± 1), k_i, which is the bimolecular inhibition rate constant is commonly employed to evaluate the inhibitory capacity of irreversible inhibitors. The bimolecular rate constant can be described as in eq 1, where [E] is the concentration of the noninhibited enzyme after a certain time, $[E_0]$ is the initial concentration of the enzyme, [I] is the concentration of the inhibitor, and t represents the time. [23]

$$\ln [E]/[E_0] = -k_i[I]t \quad (1)$$

Real sample analysis

The agriculture runoff water, collected from the paddy field (Vellore, India), was chosen as a real sample matrix to test the possible application for pesticide detection using the current method. Apple and cabbage samples, collected from a local market (Vellore, India), were also tested to

evaluate the potential of this assay for sensing pesticides in fruits/vegetables. The fruit and vegetable samples were first chopped and the edible parts of the fruits and vegetables were crushed well. Then, 10 g of each sample was mixed separately with 25 mL of Milli-Q water in a beaker, and the sample mixtures were allowed for vigorous stirring for 30 min. Then, the resulting mixture was filtered through a PES (Polyethersulfone) membrane (0.22 µm) to remove any other impurities and residue materials. Two different concentrations of trichlorfon (10^{-3} M) and malathion (10^{-3} M) were spiked in the agricultural runoff water and apple and cabbage samples. For each sample, a control sample (without spiking of trichlorfon and malathion) was also prepared using the above-mentioned procedure.

Results and discussion

The proposed mechanism for the detection of OP pesticide is expressed in the reaction scheme 1. ATCh was utilized as a substrate for the enzyme, AChE, which can catalyze the hydrolysis of ATCh into positively charged TCh (thiocholine)-bearing –SH group and acetic acid. AgNPs are formed by reduction of $AgNO_3$ by sodium borohydride ($NaBH_4$), which gets surrounded by citrate ions that adsorb onto the AgNPs surface. The generation of thiocholine molecule increases the interaction between thiol and citrate ions due to strong electrostatic force of attraction. The interparticle interactions are controlled by the thiol group, which replaces the citrate ions on the AgNPs surface. In the absence of thiol group, the AgNPs are stable, but the presence of thiol group increases the ionic strength, thereby causing the destabilization of AgNPs and increase in AgNP size during the synthesis process. When both AChE and ATCh are added to the system, thiol group gets generated by the enzymatic hydrolysis of acetothiocholine by

AChE. This thiocholine is responsible for the aggregation of AgNPs, which is also confirmed by FT–IR spectroscopy. A weak band near 2550 cm^{-1} confirms the presence of S-H group [24] of thiocholine before interaction with the NPs, which disappears after the interaction of the NPs in the presence of AChE confirming its active role in the aggregation of the particles (for details see ESI in Fig. S2). The addition of OP pesticides (trichlorfon or malathion) to the system (AChE, ATCh, $AgNO_3$, $Na_3C_6H_5O_7$, $NaBH_4$) inhibits the active site of AChE via nucleophilic attack (phosphorylation) of the serine group. As a result ATCh production is reduced consequently increasing the electrostatic repulsion between the AgNPs, and thus preventing the their aggregation.[25] With increase in concentration of OP pesticides, the production of TCh decreases significantly, there by leading to increased formation of AgNPs.

The spectral changes in the reaction mixture have been observed in the system ($AgNO_3$, $NaBH_4$, and $Na_3C_6H_5O_7$), with and without the addition of AChE and ATCh. From the UV–visible spectra in Fig. 1 (curve A), maximum absorption for AgNPs was recorded when the formation of AgNPs involved $AgNO_3$, $NaBH_4$, and $Na_3C_6H_5O_7$ alone. The addition of either AChE (in Fig. 1 curve B) or ATCh (in Fig. 1 curve C) alone to the system could not cause the aggregation of AgNPs, but only a slight decrease in the absorbance at 382 nm. This was further confirmed by measuring the particle size of the NPs using Dynamic light scattering (DLS). The addition of AChE or ATCh alone to the system gave particles of sizes, 79 ± 1 nm and 82 ± 1 nm, respectively (for details see ESI in Fig. S3). However, the addition of both AChE and ATC to the system showed a significant decrease in the absorbance at 382 nm as shown in Fig. 1 (curve D), which indicates that the addition of both AChE and ATCh to the system could cause the aggregation of AgNPs. This is because the thiocholine molecule formed can bind to the AgNPs via Ag–SR bond, which can thereby facilitate the aggregation of AgNPs.

In order to confirm the optimum concentration of AChE and ATCh required for the modulated synthesis of AgNPs, a number of control experiments were carried out as shown in Fig. 2 and 3. The effect of AChE concentration was studied by varying the concentration of AChE in the system and keeping the ATCh concentration fixed (0.1 mM). A decrease in the absorbance of the peak at 382 nm corresponding to the AChE concentration was noticed as shown in Fig. 2. The decreased absorbance of the peak was due to the aggregation of silver nanoparticles (AgNPs), which can be further confirmed by TEM. It can be seen that the maximum absorption peak was shifted slightly to a wavelength of 392 nm (red shift) when the concentration of AChE was varied from 0 to 75 mU mL^{-1}. Further, when the concentration of AChE was varied from 100 to 300 mU mL^{-1}, the absorption peak was found to shift towards the blue region. The resonance wavelength can be affected by the density of electrons, electron mass, and size of the nanoparticles (NPs).[26] The concentration of AChE (100 mU mL^{-1}) was optimized to get a maximum reaction.

Similarly, Fig. 3 shows the spectral response of the reaction mixture upon increasing the ATCh amount by keeping the AChE at a fixed concentration of 100 mU mL^{-1}. The system showed a decrease in the absorbance when the ATCh concentration was increased from 0 to 10 mM, and the system showed a maximum decrease in the absorbance peak for an ATCh concentration of 0.1 mM, and further increase in the ATCh concentration (1 and 10 mM) did not cause any significant increase in the absorbance.

The control experiments reveal that the inhibition of AChE modulated the growth of AgNPs. Based on the modulated growth of AgNPs in the presence of inhibitor, we demonstrated a sensing model to analyze the OP pesticides (trichlorfon and malathion) in aqueous solution. The addition of different wide range concentrations of trichlorfon (0.1 to 1000 nM) and malathion (1

239 to 10000 nM) to the above system increases the absorption peak at 382 nm, and their linear
240 calibration curve was plotted between different concentrations of OPs and absorbance ratio
241 (A/A_0) (Fig. 4A and 4B). The TEM analysis depicts that the absence of inhibitor in the system
242 caused the aggregation of AgNPs (Fig. 5A). The presence of OP inhibitor (10 nM of trichlorfon)
243 in the system increases the formation of AgNPs by inhibiting AChE, and the size of the AgNPs
244 was calculated with a diameter ranging from 4 to 50 nm, and the average size of the AgNPs was
245 found to be 18±1 nM (Fig. 5B).

246 The addition of OP pesticides leads to increase in the formation of AgNPs, and the prevention of
247 aggregation has been confirmed by TEM analysis. Further, the mean hydrodynamic diameter of
248 AgNPs after the addition of trichlorfon (1 nM) and malathion (1 nM) to the system in the
249 presence of AChE and ATCh were measured to be 119 ± 1 nm and 136 ± 1 nm, respectively,
250 (details are provided in ESI Fig. S4) and their zeta potential values were found to be -6.86 and -
251 8.45 mV, respectively (for details see ESI in Fig. S5).

252 In order to arrive at optimum time to measure the spectral response after adding the OPs, the
253 kinetic behavior of the enzymatic inhibition was studied closely. Fig. 6A and 6B represents the
254 kinetics of AChE inhibition by following the absorbance of the AgNPs in the presence of
255 different concentrations of trichlorfon and malathion. The decrease in enzyme activity with
256 increase in OP concentration was observed during the change in the reaction kinetics at 600 s (10
257 min). As the concentration of OP increases, the change in absorbance moves towards equilibrium
258 with increase in reaction time. The plots of absorbance (A_{382}) versus reaction time (0 to 900 s)
259 for different concentrations of OP pesticides helps to determine the concentration of noninhibited
260 AChE for further calculations of ki. By knowing the [E_0] value, we calculated the mean value of
261 ki = 6.8×10^4 M^{-1} min^{-1} and 6.7×10^3 M^{-1} min^{-1} for trichlorfon and malathion, respectively.

The sensitivity of the assay for the detection of trichlorfon and malathion was evaluated in aqueous solution. Various concentrations of trichlorfon from 0 to 1.2 nM (100 µL) were added to the reaction mixture of AChE (10 µL, 100 mU mL^{-1}) and ATCh (20 µL, 0.1 mM). The sample mixtures were incubated for 10 min at 37 °C. To these samples, a mixture of 100 µL of $AgNO_3$ (1mM), 50 µL of $Na_3C_6H_5O_7$ (1%), and 20 µL of $NaBH_4$ were added, and the final volume of the samples was diluted to 1 mL with Milli-Q water. From Fig. 7A, it can be seen that as the concentration of trichlorfon increases, the absorbance at 382 nm increases and the wavelength slightly shifts towards the red region. This is because the trichlorfon concentration may change the ionic free energy of the system, and the red-shift in the wavelength was proportional to the binding capacity of trichlorfon to the active site of AChE.[27] A good correlation (R^2 = 0.9978) was found by plotting the absorbance ratio (A/A_0) versus various concentrations of trichlorfon as shown in Fig. 7B, where A is the absorbance of the peak at 382 nm after the addition of various concentrations of trichlorfon and A_0 is the absorbance of peak at 382 nm for the control (AChE, ATCh, $AgNO_3$, $Na_3C_6H_5O_7$, and $NaBH_4$). The limit of detection (LOD) for trichlorfon was found to be 0.078 nM with a signal-to-noise ratio of 3.

Further, the sensor was developed for the determination of malathion in aqueous and real matrix solutions. In a similar way, various concentrations of malathion from 0 to 14 nM (100 µL) were added to the system with AChE and ATCh. The experimental conditions and parameters are same as that for trichlorfon. Fig. 8A shows that as the concentration of malathion increases, the maximum absorbance at 382 nm also increases. A linear dependence (R^2 = 0.9947) between the absorbance ratio (A/A_0) versus various concentrations of malathion was obtained as shown in Fig. 8B. The addition of malathion irreversibly blocks the enzyme substrate by binding to the

active site of AChE. The limit of detection (LOD) for malathion was calculated to be 2.402 nM with a signal-to-noise ratio of 3.

To validate the developed sensor for the detection of OP pesticides (trichlorfon and malathion), the analytical validation was carried out to study the accuracy of the system. All the experiments were repeated at least three times, and a detailed statistical analysis and validation (Table 1) for the enzyme-based detection of OP pesticides in aqueous solution were performed. From the obtained experimental data, the differences in the absorbance of the absorbance ratios (A/A_0) for various concentrations of trichlorfon (0 to 1.2 nM) and malathion (0 to 14 nM) were tested for statistical significance by one-way ANOVA. A p-value < 0.0001 was found for both pesticides, which ascertains the sensitivity of the system.

On the other hand, the accuracy and precision of the system were verified by performing run-to-run, day-to-day, and batch-to-batch for each trichlorfon and malathion concentrations in the range from 0.1 to 1.2 nM and 1 to 14 nM, respectively (Table 2). Table 2 indicates the high precision and accuracy of the assay.

The inhibition efficiencies (IEs) of the pesticides, trichlorfon and malathion, were further confirmed by calculating the half-maximal inhibitor concentration (IC_{50}). All the experiments were conducted in triplicates, and the IC_{50} values were statistically analyzed by non-linear regression analysis using GraphPad Prism (version 5.0) software for Windows. The two pesticides were determined to inhibit the AChE activity with IC_{50} values of 0.0241 nM and 0.1267 nM, which were obtained for trichlorfon and malathion, respectively. As the IC_{50} value indicates the inhibition efficiency of pesticide, trichlorfon and malathion will inhibit the AChE activity based on their IC_{50} values.

The efficiency of OP pesticides in inhibiting the AChE activity in real sample was performed by using the designed system. The real samples could have some negligible amount of interferences. The insoluble materials and other residues were filtered to minimize the effect of interferences on AChE during the analysis for OP pesticides. The detection of OP pesticides was monitored in the real samples like agricultural runoff water and apple and cabbage samples. A known higher concentration of trichlorfon was spiked, and the final concentrations of trichlorfon in agricultural runoff water, apple and cabbage samples were adjusted to be 0.3 and 0.6 nM. Similarly, a known higher concentration of malathion was spiked, and the final concentrations of malathion in agricultural runoff water, apple, and cabbage samples were adjusted to be 3 and 6 nM. The effect of interferences in unspiked real samples has been compared with Milli Q water and the results have been provided in Table S1 of ESI.

Each concentration of trichlorfon and malathion in real samples (agricultural runoff water, apple, and cabbage) were added separately into the reaction of mixture of AChE and ATCh, respectively, and were incubated for 10 min at 37 °C. To the resulting samples, a mixture of 100 µL of $AgNO_3$ (1 mM), 50 µL of $Na_3C_6H_5O_7$ (1%), and 20 µL of $NaBH_4$ were added, and the final volume of the samples was diluted to 1 mL with Milli-Q water. Then, the samples were analyzed with UV-visible spectroscopy, and the obtained results are summarized in Table 3 and 4. These values indicate that the designed system exhibited good recovery for the pesticides, trichlorfon and malathion, spiked in real samples.

Conclusion

In the present work, we could establish the detection of OPs by using an enzymatic substrate and by studying their effect on the formation of AgNPs produced by the addition of $AgNO_3$, $Na_3C_6H_5O_7$, and $NaBH_4$. The interaction between AChE and ATCh with the system increases the nanoparticle growth, whereas the addition of OP pesticides prevents the particle growth as corroborated from the UV–visible spectroscopy and transmission electron microscopy analyses. The developed methodology provides a very simple, low-cost, time-saving, and highly sensitive sensor for the detection of OPs in aqueous medium and real sample matrix. The sensitivity values acquired by the proposed method were 0.078 nM and 2.402 nM for trichlorfon and malathion, respectively, by colorimetric method. This method was successfully manifested for the detection of OP pesticides in spiked real samples with good recovery percentage. The described work can aid for the future development of similar colorimetric and fluorometric-based sensors for the detection of other OP and carbamate pesticides in aqueous solutions.

Acknowledgement

The authors would like to acknowledge the funding from the Defence Research & Development Organization (ERIP/ER/1103964/M/01/1485), Ministry of Defence, Government of India. We are also acknowledge the MCB department, IISc Bangalore for providing TEM facility.

References:

[1] D. E. Ray and P. G. Richards, *Toxicol. Lett*., 2001, **120**, 343–351.

[2] T. Yu, T.-Y. Ying, Y.-Y. Song, Y.-J. Li, F.-H. Wu, X.-Q. Dong and J.-S. Shen, *RSC Adv*., 2014, **4,** 8321–8327.

[3] A. L. Simonian, T. A. Good, S.-S. Wang and J. R. Wild, *Anal. Chim. Acta*, 2005, **534**, 69–77.

[4] T. Pérez-Ruiz, C. Martínez-Lozano, V. Tomás and J. Martín, *Anal. Chim. Acta*, 2005, **540**, 383–391.

[5] D. C. Paschal, R. Bicknell and D. Dresbach, *Anal. Chem*., 1977, **49**, 1551–1554.

[6] M. K. Chai and G. H. Tan, *Food Chem*., 2009, **117**, 561–567.

[7] E. Katz and I. Willner, *Angew. Chem. Int. Ed*., 2004, **43**, 6042–6108.

[8] A. Alizadeh, M. M. Khodaei, Z. Hamidi and M. B. Shamsuddin, *Sens. Actuators, B*, 2014, **190**, 782–791.

[9] F. Frederix, J.-M. Friedt, K.-H. Choi, W. Laureyn, A. Campitelli, D. Mondelaers, G. Maes and G. Borghs, *Anal. Chem*., 2003, **75**, 6894–6900.

[10] N. Xia, Q. Wang and L. Liu, *Sensors*, 2014, **15**, 499–514.

[11] M. Snejdarkova, L. Svobodova, G. Evtugyn, H. Budnikov, A. Karyakin, D. P. Nikolelis, and T. Hianik, Anal. Chim. Acta, 2004, **514**, 79–88.

[12] S. Suwansa-ard, P. Kanatharana, P. Asawatreratanakul, C. Limsakul, B. Wongkittisuksa and P. Thavarungkul, *Biosens. Bioelectron*., 2005, **21**, 445–454.

[13] A. Vakurov, C. E. Simpson, C. L. Daly, T. D. Gibson and P. A. Millner, *Biosens. Bioelectron*., 2005, **20**, 2324–2329.

[14] T.-J. Lin, K.-T. Huang and C.-Y. Liu, *Biosens. Bioelectron.,* 2006, **22**, 513–518.

[15] V. Pavlov, Y. Xiao and I. Willner, *Nano Lett*., 2005, **5**, 649–653.

[16] Y. He, B. Xu, W. Li and H. Yu, *J. Agric. Food Chem.,* 2015, **63**, 2930–2934.

[17] Z. Li, Y. Wang, Y. Ni and S. Kokot, *Sens. Actuators, B*, 2014, **193**, 205–211.

[18] G. Garai-Ibabe, L. Saa and V. Pavlov, *Analyst*, 2014, **139**, 280–284.

[19] H. M. E Azzazy, M. M. H. Mansour and S. C. Kazmierczak, *Clin. Biochem*., 2007, **40**, 917–927.

[20] J. S. Rosenthal, J. C. Chang, O. Kovtun, J. R. McBride and I. D. Tomlinson, *Chem. Biol*., 2011, **18**, 10–24.

[21] A. Virel, L. Saa and V. Pavlov, *Anal. Chem*., 2008, **81**, 268–272.

[22] Y. Wang, S. Zhang, D. Du, Y. Shao, Z. Li, J. Wang, M. H. Engelhard, J. Li and Y. Lin, *J. Mater. Chem*., 2011, **21**, 5319–5325.

[23] F. Villatte, V. Marcel, S. Estrada-Mondaca and D. Fournier, *Biosens. Bioelectron.,* 1998, **13**, 157–164.

[24] S. Aryal, B. K. C. Remant, N. Dharmaraj, N. Bhattarai, C. H. Kim and H. Y. Kim, *Spectrochim. Acta, Part A*, 2006, **63**, 160–163.

[25] R. T. Delfino and J. D. Figueroa-Villar, *J. Phys. Chem. B,* 2009, **113**, 8402–8411.

[26] Y.-W. Ma, Z.-W. Wu, L.-H. Zhang, J. Zhang, G.-S. Jian and S. Pan, *Plasmonics*, 2013, **8**, 1351–1360.

[27] J. P. Walker and S. A. Asher, *Anal. Chem*., 2005, **77**, 1596–1600.

[28] D. Du, J. Ding, Y. Tao and X. Chen, *Sens. Actuators, B*, 2008, **134**, 908–912.

[29] M. Liang, K. Fan, Y. Pan, H. Jiang, F. Wang, D. Yang, D. Lu. J. Feng, J. Zhao, L. Yang and X. Yan, *Anal. Chem*., 2013, **85**, 308–312.

[30] D. Du, J. Ding, J. Cai and A. Zhang, *Sens. Actuators, B*, 2007, **127**, 317–322.

[31] G. Liu and Y. Lin, *Anal. Chem.*, 2005, **77**, 5894–5901.

List of figures

Scheme 1. Detection of acetylcholinesterase-based inhibitors during the synthesis of silver nanoparticles.

Fig. 1. UV–visible spectra of AgNPs grown in the system containing $AgNO_3$ (1 mM), $Na_3C_6H_5O_7$ (1 %), and $NaBH_4$ (10 mM), in presence and absence of AChE (100 mU mL^{-1}) and ATCh (0.1 mM).

Fig. 2. UV–visible spectra of AgNPs formed in presence of $AgNO_3$ (1 mM), $Na_3C_6H_5O_7$ (1 %), $NaBH_4$ (10 mM), and ATCh (0.1 mM) and various concentrations of AChE (0–300 mU mL^{-1}).

Fig. 3. UV–visible spectra of AgNPs produced in presence of $AgNO_3$ (1 mM), $Na_3C_6H_5O_7$ (1 %), $NaBH_4$ (10 mM), AChE (100 mU mL^{-1}) and various concentrations of ATCh (0–10 mM).

Fig. 4. Linear calibration curve plotted with absorption ratios against different concentrations of A) trichlorfon B) malathion.

Fig. 5. TEM images of **A)** AgNPs aggregated in presence of $AgNO_3$ (1 mM), $Na_3C_6H_5O_7$ (1 %), $NaBH_4$ (10 mM), AChE (100 mU mL^{-1}), and ATCh (0.1 mM) and **B)** AgNPs formed in presence of ATCh (0.1 mM), AChE (100 mU mL^{-1}), and trichlorfon (10 nM), added to the system containing $AgNO_3$ (1 mM), $Na_3C_6H_5O_7$ (1 %), and $NaBH_4$ (10 mM).

Fig. 6. Kinetic behavior of AgNP formation in presence of AChE (100 mU mL^{-1}) and ATCh (0.1 mM) with various concentrations of **A)** trichlorfon (0 to 1.0 nM) and **B)** malathion (0 to 10 nM). In all experiments, the system contained $AgNO_3$ (1 mM), $Na_3C_6H_5O_7$ (1 %), and $NaBH_4$ (10 mM).

412 **Fig. 7. A)** UV–visible spectra of AgNPs formed in presence of $AgNO_3$ (1 mM), $Na_3C_6H_5O_7$ (1
413 %), $NaBH_4$ (10 mM), ATCh (0.1 mM), and AChE (100 mU mL^{-1}) with various concentrations
414 of trichlorfon (0 to 1.2 nM) and **B)** Calibration curve for the analysis of trichlorfon.

415 **Fig. 8. A)** UV–visible spectra of AgNPs formed in presence of $AgNO_3$ (1 mM), $Na_3C_6H_5O_7$ (1
416 %), $NaBH_4$ (10 mM), ATCh (0.1 mM), and AChE (100 mU mL^{-1}) with various concentrations
417 of malathion (0 to 14 nM) and **B)** Calibration curve for the analysis of malathion.

418

419

List of Tables

425 **Tables:**

426 **Table 1.** Comparison of the LODs for OPs with reported references and current work.

Employing nanoparticles	OPs	LOD [a]	Ref.
CdTe quantum dots (QDs) [b]	Paraoxon	8 nM	2
Chitosan-AuNPs [c]	Malathion	0.1 nM	28
Fe_3O_4 Magnetic Nanoparticle	Sarin, methyl-paraoxon, acephate	1 nM, 10 nM, 5000 nM	29
AuNPs-chitosan as template [d]	Malathion	0.09 nM	30
ZrO_2 NPs [d]	Methyl parathion	3.432 nM	31
During synthesis of AgNPs in presence of AChE and ATCh [e]	Trichlorfon, malathion	0.078 nM, 2.402 nM	Present work

427

428 *a*: Limit of detection.

429 *b*: Photoluminescence method.

430 *c*: Cyclic voltammogram (CV) method .

431 *d*: Electrochemical method.

432 *e*: System included $AgNO_3$, $Na_3C_6H_5O_7$, and $NaBH_4$.
433

434 **Table 2.** Statistical analysis for detection of trichlorfon and malathion.

Analyte	Linear regression [a]	R^2 [b]	Linear range (nM)	LOD [c] (nM)	RSD [d] % (n=3)		
					Run-to-Run	Day-to-Day	Batch-to-Batch
Trichlorfon	$Y = 0.8864x + 1.0434$	0.9978	0.1 to 1.2	0.078	3.6	2.5	5.2
Malathion	$Y = 0.0288x + 1.1342$	0.9947	1 to 14	2.402	3	5.1	4.5

435 *a*: Linear regression equation; Y = relative absorbance (A/A_0); x = logarithmic concentration of
436 trichlorfon and malathion

437 *b*: The coefficient of determination.

438 *c*: Limit of detection.

439 *d*: Relative standard deviation measured from 3 parallel experiments.

440

441 **Table 3.** Detection of trichlorfon in spiked real samples.

Sample	Added (nM)	Found (nM)	Recovery (%)	RSD (%)
Agricultural runoff water	0.3	0.3	100.0	2.1
	0.6	0.59	98.33	3.9
Apple	0.3	0.32	106.67	1.3
	0.6	0.56	93.33	1.8
Cabbage	0.3	0.28	93.33	0.4
	0.6	0.57	95.00	0.7

442

443 **Table 4.** Detection of malathion in spiked real samples.

Sample	Added (nM)	Found (nM)	Recovery (%)	RSD (%)
Agricultural runoff water	3	2.6	86.67	0.24
	6	6.4	106.67	0.19
Apple	3	2.7	90.0	0.33
	6	6.3	105.0	0.22
Cabbage	3	2.8	93.33	0.71
	6	6.2	103.33	0.53

444

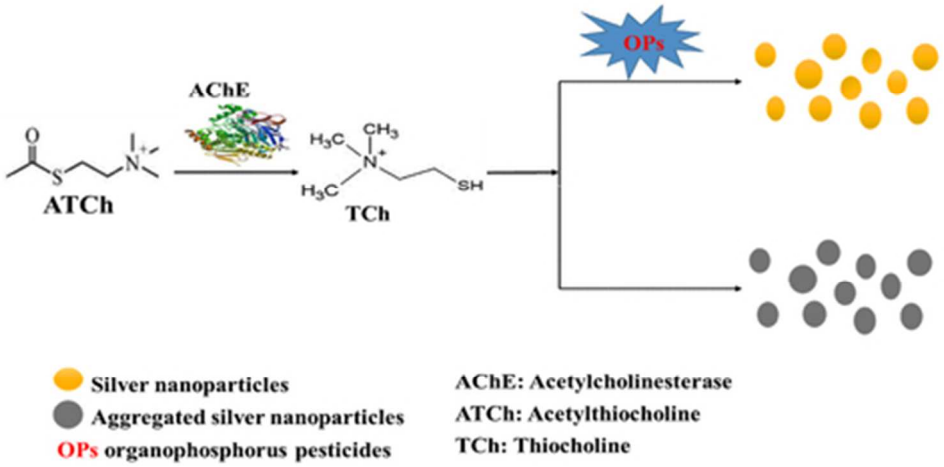

39x19mm (300 x 300 DPI)

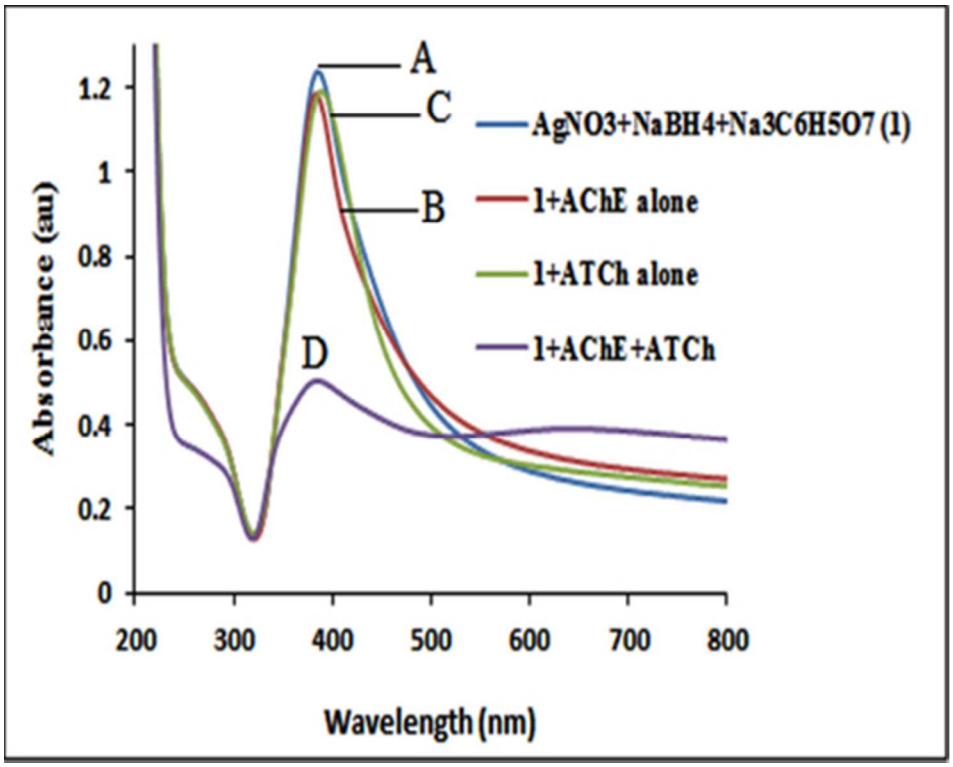

Figure 1
39x32mm (300 x 300 DPI)

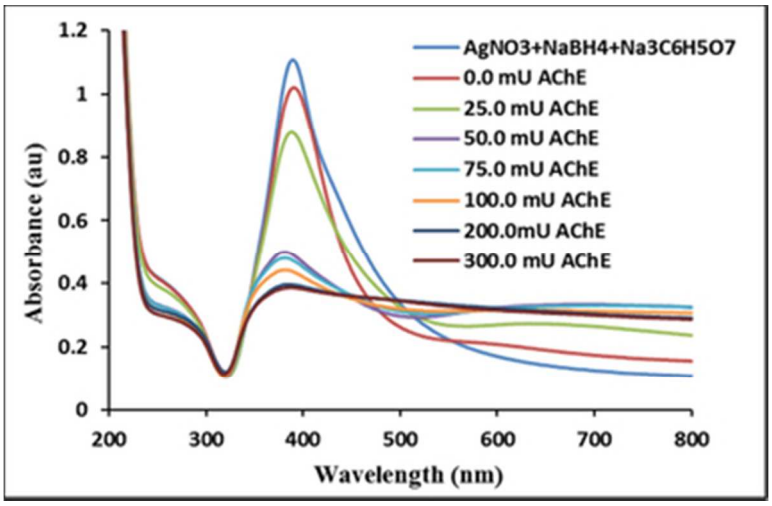

Figure 2
32x20mm (300 x 300 DPI)

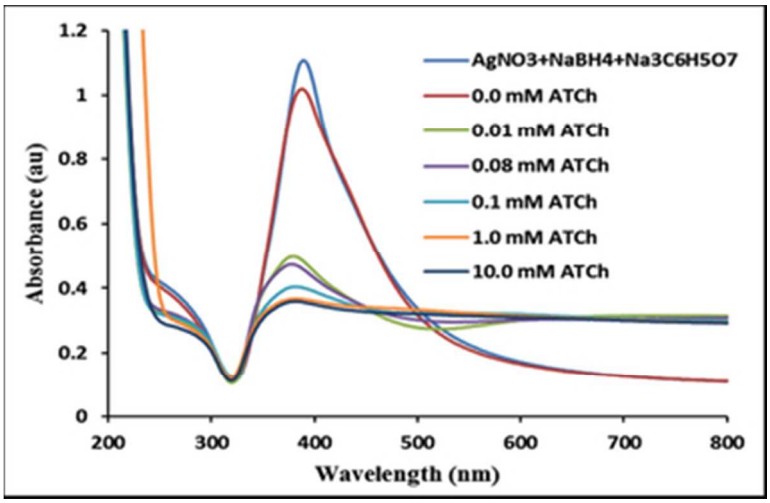

Figure 3
32x20mm (300 x 300 DPI)

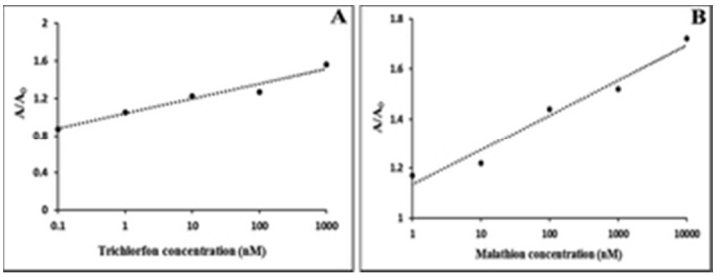

Figure 4
29x11mm (300 x 300 DPI)

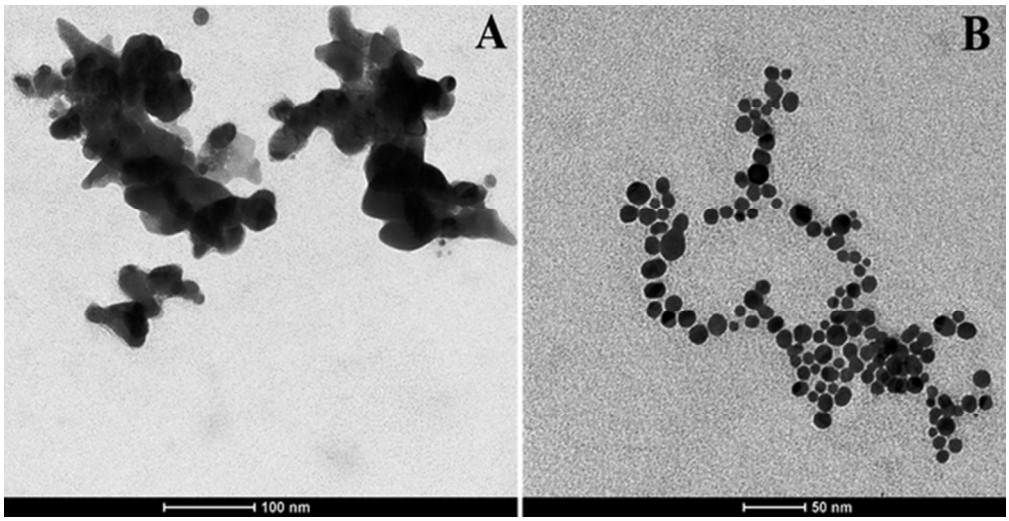

Figure 5
53x27mm (300 x 300 DPI)

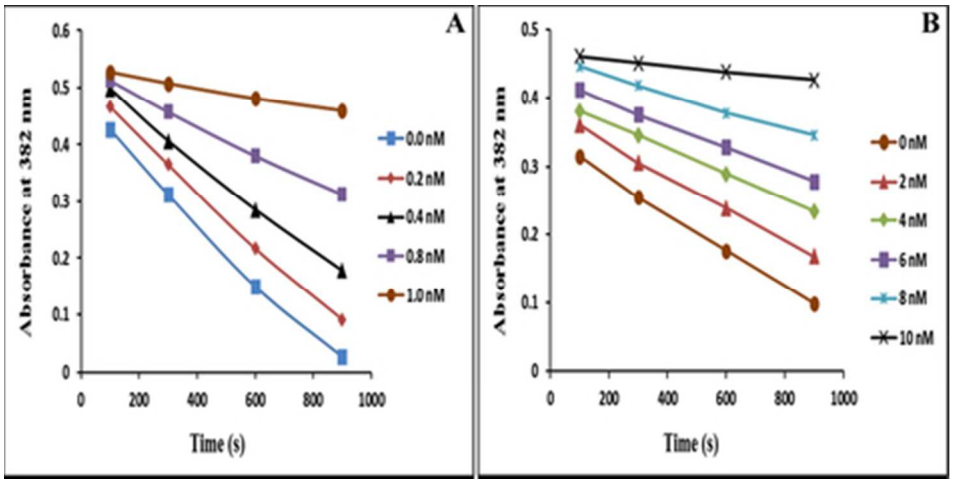

39x19mm (300 x 300 DPI)

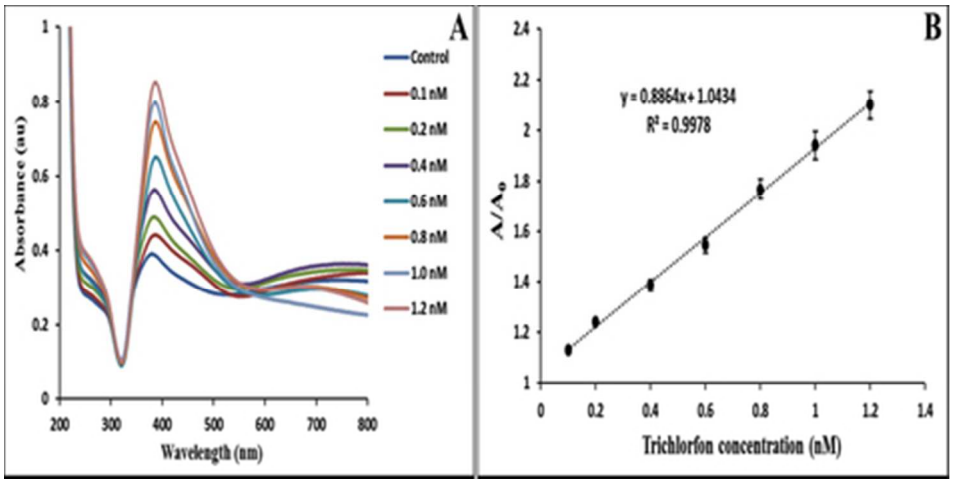

39x19mm (300 x 300 DPI)

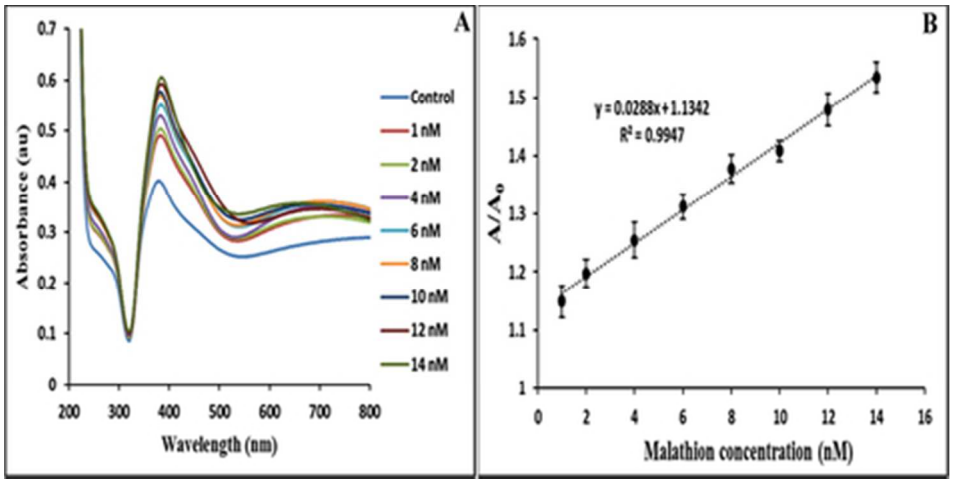

39x19mm (300 x 300 DPI)